

1 **Meaning maps and saliency models based on deep**
2 **convolutional neural networks are insensitive to image**
3 **meaning when predicting human fixations**

4
5
6 **Marek A. Pedziwiatr¹***, Matthias Kümmerer², Thomas S.A. Wallis^{2, 3}, Matthias Bethge²,
7 **Christoph Teufel¹**

8
9 ¹Cardiff University, Cardiff University Brain Research Imaging Centre (CUBRIC), School of Psychology
10 Cardiff, United Kingdom

11 ²University of Tübingen, Center for Integrative Neuroscience, Tübingen, Germany

12 ³Bernstein Center for Computational Neuroscience, Tübingen, Germany

13
14 *Corresponding author: marek.pedziwi@gmail.com

15
16 **Abstract**

17 Eye movements are vital for human vision, and it is therefore important to understand how
18 observers decide where to look. Meaning maps (MMs), a technique to capture
19 the distribution of semantic importance across an image, have recently been proposed to
20 support the hypothesis that meaning rather than image features guide human gaze. MMs
21 have the potential to be an important tool far beyond eye-movements research. Here, we
22 examine central assumptions underlying MMs. First, we compared the performance of MMs
23 in predicting fixations to saliency models, showing that DeepGaze II – a deep neural network
24 trained to predict fixations based on high-level features rather than meaning – outperforms
25 MMs. Second, we show that whereas human observers respond to changes in meaning
26 induced by manipulating object-context relationships, MMs and DeepGaze II do not.
27 Together, these findings challenge central assumptions underlying the use of MMs to
28 measure the distribution of meaning in images.

29 Keywords: eye movements, natural scenes, saliency, deep neural networks, meaning maps

Pedziwiatr et al.

30

Introduction

31 Human eyes resolve fine detail only in a small, central part of the visual field, with resolution
32 dropping off rapidly in the periphery. To sample details, we move our eyes to orient the high-
33 resolution part of our visual system successively to different parts of a visual scene.
34 Information about these small scene parts is extracted during fixations – short periods in
35 which the eyes are relatively stable. Thus, due to the structure of our visual system, human
36 vision depends on eye movements. How the brain decides where to look in a visual scene is
37 therefore an important question. A long-standing hypothesis suggests that semantic content
38 of image regions is important in guiding eye movements. Recent work presented meaning
39 maps (MMs) as a tool to test this hypothesis (Henderson & Hayes, 2017, 2018). This technique
40 aims to index the spatial distribution of meaning across an image, which has potential
41 applications far beyond eye-movement research. Here, we assess and challenge central
42 assumptions of this novel tool.

43 A classic finding in eye-movement research shows that the specific task of an observer has an
44 influence on where they direct their eyes (Yarbus, 1967; Hayhoe & Ballard, 2005). But in
45 everyday life, we frequently move our eyes without any goal other than to explore the
46 environment. In the lab, this behavior is examined in free-viewing paradigms, during which
47 eye movements are recorded while images are viewed without an explicit task (Koehler, Guo,
48 Zhang, & Eckstein, 2014, but see Tatler, Hayhoe, Land, & Ballard, 2011). To explain what
49 guides eye movements during free viewing, two opposing accounts have been put forward.

50 According to the first account, eye movements are guided primarily by image characteristics
51 (Borji, Sihite, & Itti, 2013; Itti & Koch, 2001; Parkhurst, Law, & Niebur, 2002). Potential support
52 for this view comes from saliency models: algorithms, which exclusively use visual features of
53 an image to predict human fixations. Although early models, which used only simple features
54 such as local intensity or colors (Itti & Koch, 2000), are now deemed only moderately
55 successful (Bylinskii et al., 2014), more recent saliency models achieve a remarkably high
56 performance (Kümmerer, Wallis, Gatys, & Bethge, 2017). These models harness deep
57 convolutional neural networks – biologically inspired machine learning algorithms, that
58 somewhat resemble the human visual system (Kietzmann, McClure, & Kriegeskorte, 2019).
59 However, even such models rely solely on visual features, albeit high-level ones.

Pedziwiatr et al.

60 In contrast to the idea underlying saliency models, several authors have argued that during
61 free viewing, eye movements are mainly guided by the semantic content of the visual scene
62 (Henderson, Malcolm, & Schandl, 2009; Nyström & Holmqvist, 2008; Onat, Açık, Schumann,
63 & König, 2014; Rider, Coutrot, Pellicano, Dakin, & Mareschal, 2018; Stoll, Thrun, Nuthmann,
64 & Einhäuser, 2015). This perspective differs fundamentally from the saliency-based approach.
65 Attributing meaning to certain parts of the scene is impossible without prior knowledge of
66 the world, i.e., a factor that is independent of the visual input (Hegde & Kersten, 2010; Teufel,
67 Dakin, & Fletcher, 2018). Consequently, the notion that semantic content guides eye-
68 movements is inconsistent with the idea that the allocation of fixations is dependent solely
69 on the distribution of image features. Given that meaning is not image-computable, the
70 notion that semantic content guides eye-movements is inconsistent with the idea that the
71 eye-movements are dependent solely on the distribution of image features.

72 A string of recent studies has claimed to provide support for the role of meaning in driving
73 eye movements (Hayes & Henderson, 2019; Henderson & Hayes, 2017, 2018; Henderson,
74 Hayes, Rehrig, & Ferreira, 2018; Peacock, Hayes, & Henderson, 2018). These studies
75 (reviewed in Henderson, Hayes, Peacock, & Rehrig, 2019) are based on a novel technique
76 called meaning maps (MMs). A MM for a given image is created by breaking it down into small
77 isolated patches, which are rated for their meaningfulness independently from the rest of the
78 visual scene. These ratings are pooled together into a smooth map, which is supposed to
79 capture the distribution of meaning across the image. Compared to outputs from a simple
80 saliency model (GBVS, Harel et al., 2006), MMs were more predictive of human fixations. On
81 that basis it has been claimed that meaning guides human fixations in natural scene viewing
82 (Henderson & Hayes, 2017, 2018). Here, we examined central predictions of this claim.

83 First, if MMs measure meaning and if meaning guides human eye-movements, MMs should
84 be better in predicting locations of fixations than saliency models because these models rely
85 solely on image features. Therefore, we compared MMs to a range of classic and state-of-the-
86 art models. We replicate the finding that MMs perform better than some of the most basic
87 saliency models. Contrary to the prediction, however, DeepGaze II (DGII; Kümmeler, Wallis,
88 & Bethge, 2016; Kümmeler et al., 2017), a model based on a deep convolutional neural
89 network, outperforms MMs.

Pedziwiatr et al.

90 A second prediction is that if MMs are sensitive to meaning and if meaning guides human
91 gaze, differences in eye movements that result from changes in meaning should be reflected
92 in equivalent differences in MMs. We probed this prediction experimentally using a well-
93 established effect: the same object, when presented in an atypical context (e.g., a shoe on a
94 bathroom sink) attracts more fixations than when presented in a typical context because of
95 the change in the semantic object-context relationship (Henderson, Weeks, & Hollingworth,
96 1999; Öhlschläger & Võ, 2017). Replicating previous studies, image regions attracted more
97 fixations when they contained context-inconsistent compared to context-consistent objects.
98 Crucially, however, MMs of the modified scenes did not attribute more 'meaning' to these
99 regions. DGII also failed to adjust its predictions accordingly.

100 Together, these findings suggest that semantic information contained in visual scenes is
101 critical for the control of eye movements. However, this information is captured neither by
102 MMs nor DGII. We suggest that similar to saliency models, MMs index the distribution of
103 visual features rather than meaning.

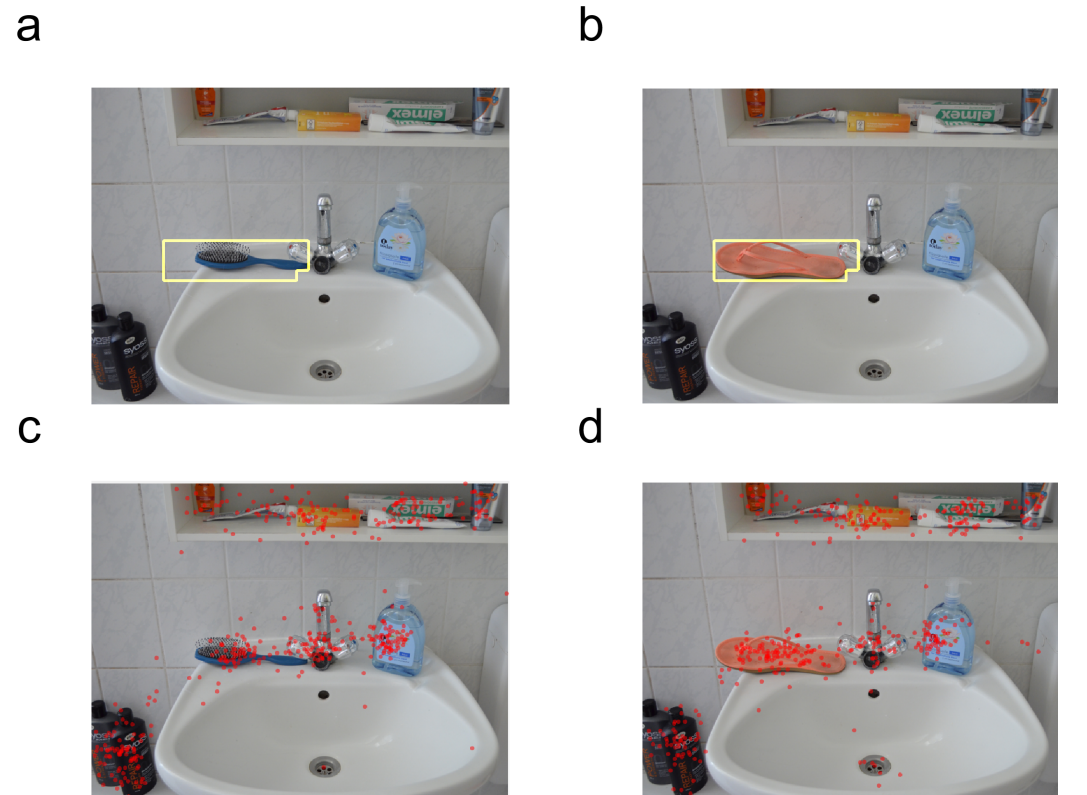
104

105

Method

106 We conducted a single experiment in which human observers free-viewed natural scenes
107 while their eye-movements were being recorded. The obtained data was analyzed in two
108 complimentary ways. First, we compared how well MMs and different saliency models predict
109 locations of human fixations in natural scenes. Subsequently, we assessed the sensitivity of
110 MMs and the best-performing saliency model to manipulations of scene meaning. The
111 reported experiment was not preregistered. The data, the code to create MMs, and all openly
112 available resources used in the study can be accessed via the links provided in the
113 Supplement.

Pedziwiatr et al.



114

115 Fig. 1. Illustration of sample stimuli in (a) the Consistent and (b) the Inconsistent condition
116 with the Critical Region outlined in yellow and (c, d) human fixations recorded in both
117 conditions. In this example, a hair brush on a bathroom sink (a) – an object consistent with
118 the scene context – has been exchanged for a shoe (b) to introduce semantic inconsistency.

119

120 **Stimuli.** We used images from two conditions of the SCEGRAM database (Öhlschläger & Võ,
121 2017): the Consistent and the Semantically Inconsistent conditions (called ‘Inconsistent’
122 here). In the Consistent condition (used in both analyses), scenes contain only objects that
123 are typical for a given context. In the Inconsistent condition (used only in the second analysis),
124 one of the objects is contextually inconsistent. For example, a hairbrush in the context of a
125 bathroom sink from the Consistent condition is replaced with a flip-flop in the Inconsistent
126 condition (see Figs. 1a and 1b). Such changes in object-context relationship alter the meaning
127 attached to the manipulated object. For every scene, we indexed the location of the
128 consistent and inconsistent objects with the superimposed bounding boxes for both objects
129 (see Figs. 1a and 1b). We refer to this location as the Critical Region, because it is the only
130 part of the image that changes between Consistent and Inconsistent conditions. We used 36
131 selected scenes in both conditions (72 photographs in total, listed in the Supplement together

Pedziwiatr et al.

132 with the selection criteria). We also replicated the main finding of the first analysis in an
133 additional set of 30, very different, images (reported in the Supplement).

134

135 **Procedure.** The procedure consisted of 3 blocks, interleaved with breaks. Participants were
136 instructed to 'look carefully at each' image. Experimental blocks began with an eye tracker
137 calibration/validation. Within each block, observers free-viewed a series of 24 photographs
138 from both SCEGRAM conditions, each for 7 seconds. After image offset, observers were
139 required to press a button to view the next image. Then, a fixation point appeared centrally
140 on a screen and once observers fixate on it (as determined online by their eye-trace), the
141 actual image was displayed. Before starting the experiment, observers viewed a sample image
142 in an identical regime to familiarize themselves with the procedure. Each stimulus was shown
143 once and the order of presentation was fully randomized. The stimuli were presented against
144 a uniform grey background and had a width of 688 pixels and a height of 524 pixels, which
145 subtended approximately 19.7 and 15 degrees of visual angle, respectively. Stimulus
146 presentation time and size were adopted from a previous study with the SCEGRAM database
147 (Öhlschläger & Vö, 2017).

148

149 **Observers.** 20 volunteers (3 male; mean age 19.4) recruited from the Cardiff University
150 undergraduate population took part in the study. All reported normal or corrected-to-normal
151 vision, provided written consent, and received course credits in return for participation. The
152 study was approved by the Cardiff University School of Psychology Research Ethics
153 Committee. The primary units of interest in our analyses were the distributions of fixations
154 over images. The number of observers we recruited guarantees that including more observers
155 would not change these distributions significantly (demonstrated in the Supplement).

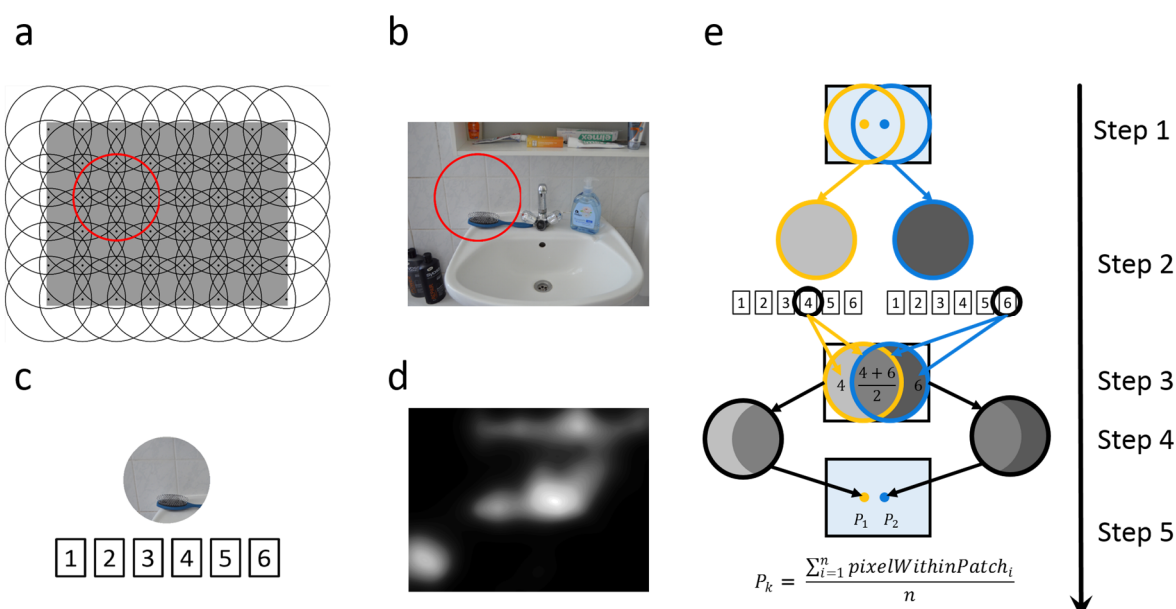
156

157 **Apparatus.** The study was conducted in a dimly lit room. SCEGRAM images from both
158 conditions were presented on an LCD monitor (Iiyama ProLite B2280HS, resolution 1920 by
159 1080 pixels, 21 inches diagonal). Chin and forehead rests were used to ensure that observers
160 maintained the constant distance of 49 cm from the screen. Their eye movements were

Pedziwiatr et al.

161 recorded with the frequency of 500 Hz using an EyeLink 1000+ eye tracker placed on a tower
162 mount. The experiment was controlled by custom-written Matlab (R2017a version) scripts
163 using Psychophysics Toolbox Version 3 (Kleiner, Brainard, & Pelli, 2007).

164



165

166 Fig. 2. Illustration of the stimuli and procedure used for creating meaning maps. (a) Grids of
167 equally spaced circles were used to cut images into fine and coarse patches (only the latter
168 are illustrated here). The red circle indicates a sample patch in the grid. (b) Here, the sample
169 patch is highlighted in one of the scenes from the Consistent condition. (c) Patches were
170 presented in isolation and rated for their meaningfulness by three independent observers on
171 a scale from 1 to 6. The panel has illustrative purpose only – the scale presented to observers
172 included additional labels (ranging from 'Very Low' to 'Very High'). (d) Illustration of a
173 meaning map with greyscale values indicating 'meaningfulness'. (e) Simplifying illustration of
174 how meaning maps are generated from ratings. For simplicity sake, only two patches are
175 shown (step 1). Each patch is rated in isolation (step 2; here only one rating per patch is
176 shown). All pixels within an image area are then assigned average rating values, taking into
177 account all ratings for patches that overlap with this area (step 3). For the area of the original
178 patch (step 4), all pixels are then averaged and the resulting value is assigned to the center of
179 the patch (step 5). Finally, the patch centers were used as interpolation nodes for thin-plate
180 spline interpolation producing a smooth distribution of values over the image (not illustrated).

Pedziwiatr et al.

181 This procedure was conducted separately for the fine and coarse grid, and the meaning map
182 for a given image was created by averaging the two outcomes and normalizing the result to a
183 range between 0 and 1.

184

185 **Creating MMs.** To create MMs for our stimuli, we followed the procedure described by
186 Henderson & Hayes (2017, 2018; for details see Fig. 2). Each image was segmented into
187 partially overlapping patches of two sizes: fine patches had a diameter of 107 pixels (3 degrees
188 of the visual angle, or 16 % of the image width), coarse patches of 247 pixels (7 degrees or
189 36% of the image width) (Fig. 2a and b). Their centers were 58 pixels (fine) and 97 pixels
190 (coarse) apart from each other.

191 Next, we collected meaningfulness ratings from human subjects for all patches. Each patch
192 was presented in isolation and rated for its meaningfulness on a 6 point Likert scale (Fig. 2).
193 As in Henderson and Hayes (2017), we used a Qualtrics survey completed by naive observers
194 recruited via the crowdsourcing platform Amazon Mechanical Turk (see Supplement for
195 eligibility criteria). Each participant provided ratings for 305 or 303 patches of both sizes
196 (selected randomly from all images), on average spent approximately 14 min on the task, and
197 received 2.18 USD as remuneration. In total, 69 individuals were used as raters, with three
198 individuals rating each individual patch. The collected ratings were then used to create MMs
199 (see Fig. 2).

200 When creating MMs for images from both conditions, we exploited the fact that photographs
201 from the Consistent and Inconsistent conditions differ only in the Critical Region (the part of
202 the image containing the manipulated object) while the remaining parts overlap. We
203 collected meaningfulness ratings for the patches belonging to overlapping areas only once,
204 and the separate sets of ratings for Consistent and Inconsistent condition were collected only
205 for those patches that contained at least one pixel belonging to the Critical Region. In total,
206 the number of patches rated in the study amounted to 7013: 4840 fine patches (of which 520
207 belonged to the images from the Inconsistent condition) and 2173 coarse patches (445
208 Inconsistent).

209

Pedziwiatr et al.

210 **Saliency models.** In the first analysis, we compared predictive performance of MMs to four
211 saliency models of different complexity. The first two models – GBVS (Harel et al., 2006) and
212 AWS (Garcia-Diaz, Fdez-Vidal, Pardo, & Dosil, 2012) – rely on simple visual features, such as
213 local colors and edge orientations, and share the assumption that fixations land on image
214 regions distinct from their surroundings in terms of values of these features. By contrast to
215 GBVS, AWS includes a statistical whitening procedure to improve performance. Both these
216 models were previously used to estimate the influence of image features relative to cognitive
217 factors on the deployment of fixations: GBVS in the previous studies with MMs, AWS
218 elsewhere (Stoll et al., 2015).

219 Two other models that we compared to MMs – ICF and DeepGaze II (DGII) – were designed
220 in a data-driven manner (Kümmerer et al., 2017). Both have the same architecture, consisting
221 of a fixed network that extracts sets of features from images and a readout network that is
222 trained on human fixations separately for each model to combine the features in a way to
223 maximize the models' predictive power. While the fixed network of ICF extracts only simple
224 visual features (local intensity and contrast), DGII is tuned to features extracted by a deep
225 convolutional neural network pre-trained for object recognition (VGG-19; Simonyan &
226 Zisserman, 2014).

227 All saliency models output smooth maps that predict the probability of image regions to be
228 fixated. Human observers have the tendency to look at the center of images (Tatler, 2007),
229 and therefore this probability is usually higher in the central region of the image. This 'center
230 bias' has important consequences for the evaluation of saliency models. Their performance
231 differs depending on whether they are evaluated using a metric expecting some form of this
232 bias or not (Kümmerer, Wallis, & Bethge, 2018). Here, for the sake of simplicity, we do not
233 incorporate center bias in the models or in the MMs (unlike the original authors) and use an
234 appropriate metric for this situation (see Performance metrics section). Importantly, analyses
235 addressing the issue of center bias in a more extensive way (reported in the Supplement)
236 provide only further support for our conclusions.

237

238 **Data pre-processing.** Fixation locations from the eye tracker recordings were extracted using
239 the algorithm provided by the device manufacturer operating with the default parameter

Pedziwiatr et al.

240 values. Thereby, we obtained a discrete distribution of fixations on each image (see Fig. 1c
241 and 1d). Then, in line with the previous MMs studies, we smoothed these discrete
242 distributions with a Gaussian filter with a cutoff frequency of -6 dB, using the function
243 provided by Bylinskii and colleagues (2014).

244 Next, smooth distributions from fixations, models, and MMs were separately normalized to a
245 range from 0 to 1 for each image. Finally, for each scene, histograms of all distributions from
246 both conditions were matched to histograms of smoothed fixations from Consistent condition
247 using the Matlab imhistmatch function, as in the original MMs studies. Histogram matching
248 makes distributions directly comparable as it ensures that they differ only with respect to
249 their shape, and not their total mass.

250

251 **Performance metrics.** To compare the ability of MMs and models to predict locations of
252 human fixations in Experiment 1, we use two well-established metrics (Bylinskii, Judd, Oliva,
253 Torralba, & Durand, 2016): Correlation and Shuffled Area Under ROC curve (sAUC; Zhang,
254 Marks, Tong, Shan, & Cottrell, 2007) with the implementations provided by Bylinskii and
255 colleagues (2014).

256 Correlation, used in the previous studies on MMs, is calculated as Pearson's linear correlation
257 coefficient between a smoothed distribution of observers' fixations over the image and
258 predictions of a saliency model or MMs. We additionally used sAUC (Zhang et al., 2008),
259 which, unlike Correlation, guarantees that the measured differences in performance between
260 models are driven by their sensitivity to factors guiding fixations, and not by the degree to
261 which they include human center bias in their predictions, even implicitly (Kümmerer, Wallis,
262 & Bethge, 2015; Kümmerer et al., 2018).

263

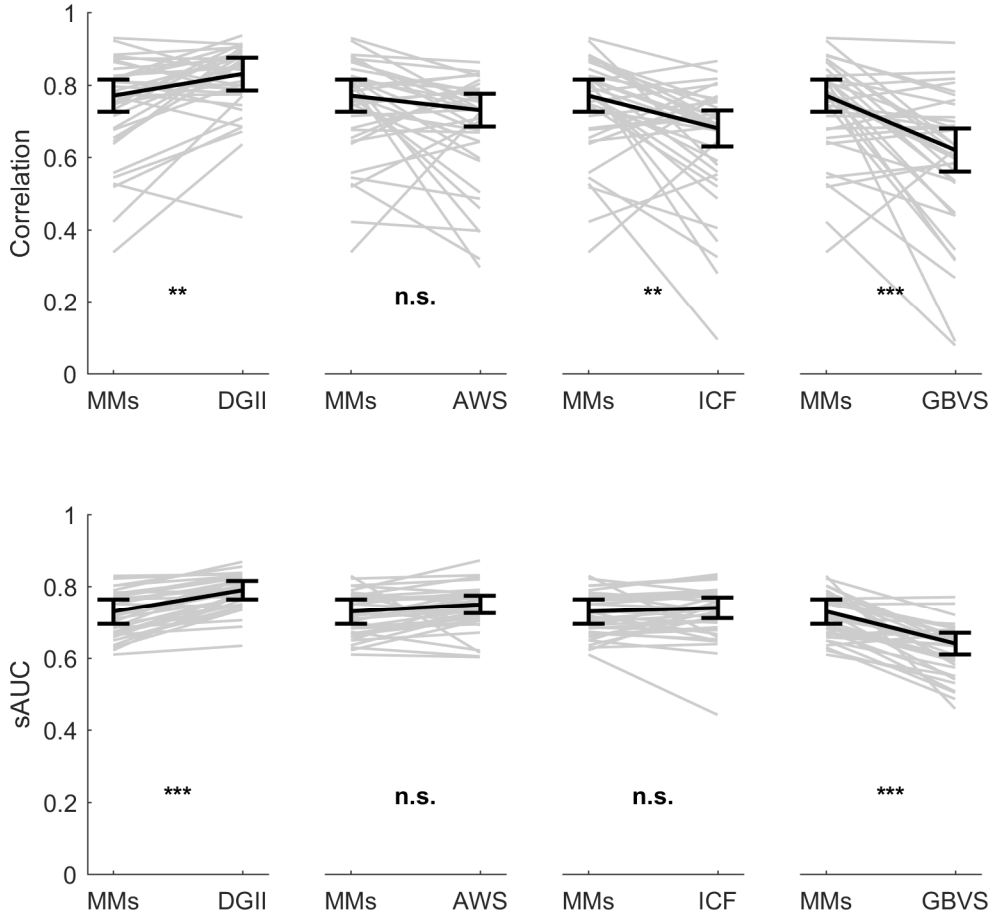
264 **Comparing meaning maps and saliency models – results**

265 In the first analysis, we compared performance of four saliency models to MMs in predicting
266 human fixations in the Consistent condition, i.e., when viewing typical scenes with no obvious
267 object-context inconsistencies (Tab. 1, Fig. 3). If human gaze is guided by meaning, and if MMs

Pedziwiatr et al.

268 provide an index for the distribution of meaning, we would expect MMs to outperform all
269 saliency models because these models are based solely on image features.

270



271

272

273 Fig. 3. Performance of MMs and saliency models in predicting human fixations according to
274 (a) Correlation and (b) sAUC metrics. Note that according to both metrics DGII predicted
275 human fixations better than MMs. Asterisks indicate p-values from statistical tests comparing
276 MMs to different models (reported in Table 1.): * indicates $p \leq .05$, ** $p \leq .01$, *** $\leq .001$ and
277 'n.s.' indicates the lack of statistical significance. Grey lines connect values obtained for
278 individual images. Black vertical bars indicate 95% confidence intervals for the medians.

279

280 **Predictive power.** Correlation and sAUC values obtained for MMs and for each of the models
281 were compared using Bonferroni-corrected paired Wilcoxon tests (Fig. 3; Tab. 1). We used
282 non-parametric tests because for some of the distributions the assumptions of normality was

Pedziwiatr et al.

283 not met. For the same reason we chose a median as a measure of centrality (we calculate
284 confidence intervals for median using a bootstrapping method – see details in the
285 Supplement). Additionally, we calculated JZS Bayes Factor (Rouder, Speckman, Sun, Morey, &
286 Iverson, 2009) to quantify the evidence for (or against) the differences between models and
287 MMs (Tab. 1). While deviations from normality can be problematic for Bayes factor analyses,
288 they are most likely not an issue in the current situation: the Bayes factors for the key finding
289 are large and the deviations from normality are small.

290 As shown in Tab. 1 and on Fig. 3, according to both measures, MMs outperformed GBVS in
291 predicting human fixations, thereby replicating the results of Henderson and Hayes (2017,
292 2018) using new images and new participants. Contrary to expectations, however, both
293 metrics indicated that DGII predicted fixations better than MMs. Furthermore, performance
294 of AWS and MMs did not differ significantly irrespective of the metrics. Finally, MMs
295 outperformed ICF according to Correlation, but not sAUC. In fact, for the latter metric, JZS-
296 Bayes Factor indicated support for the null hypothesis.

297

298 Table 1. Comparison of Predictive Power of Saliency Models and MMs Using Correlation and
299 sAUC.

Model	Median of prediction values with 95% confidence intervals	Median of differences from MMs with 95% confidence intervals	Z statistic	p-value (Bonferroni-corrected)	JZS Bayes Factor
Correlation					
DGII	0.83 [0.78, 0.87]	0.07 [0.03, 0.11]	-3.11	0.00738	32.26
MMs	0.77 [0.72, 0.81]	–	–	–	–
AWS	0.73 [0.67, 0.76]	-0.06 [-0.12, -0.01]	-2.23	0.10412	1.48
ICF	0.68 [0.61, 0.71]	-0.12 [-0.18, -0.06]	-3.04	0.00936	16.90
GBVS	0.62 [0.56, 0.68]	-0.11 [-0.26, -0.05]	-3.97	< .001	396.96
sAUC					
DGII	0.79 [0.77, 0.82]	0.06 [0.05, 0.08]	-6.36	< .001	> 1000
MMs	0.73 [0.69, 0.76]	–	–	–	–
AWS	0.75 [0.72, 0.77]	0.02 [0.01, 0.04]	-2.49	0.0507	0.60
ICF	0.74 [0.70, 0.76]	0.01 [-0.01, 0.02]	-0.77	1.00	0.19
GBVS	0.64 [0.60, 0.66]	-0.10 [-0.12, -0.08]	-5.96	< .001	> 1000

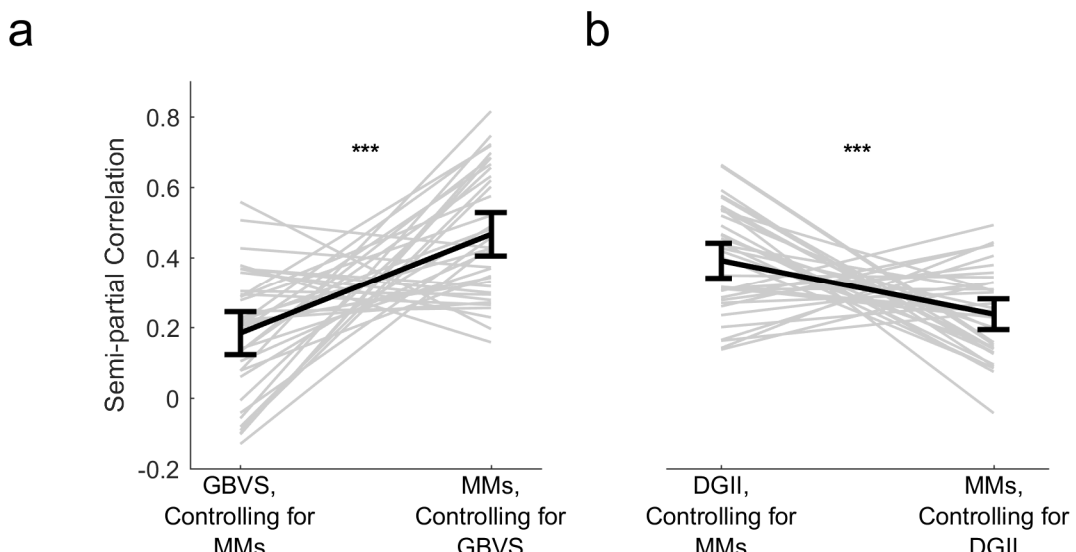
Pedziwiatr et al.

300

301 **Semi-partial correlations.** Because predictions of models and MMs overlap, we quantified
302 their distinct predictive power using semi-partial correlations. We conducted these analyses
303 for GBVS (used in the original MMs studies) and DGII (the only model which markedly
304 outperformed MMs).

305 For each scene from the Consistent condition, we calculated two semi-partial correlations
306 with the distribution from smoothed fixations: one for MMs while controlling for GBVS, and
307 one for GBVS while controlling for MMs (see Fig. 4). Consistent with findings by Henderson
308 and Hayes (2018), MMs explain more unique variance than GBVS (Fig. 6a), as indicated by the
309 significantly higher coefficients in the former than the latter case (mean difference 0.28, 95%
310 confidence interval (CI) [0.17, 0.39]; paired t-test, $t(35) = 5.22$, $p < .001$). Interestingly, the
311 identical analysis with DGII revealed that DGII explained significantly more unique variance
312 than MMs (mean difference 0.15, 95% CI [0.07, 0.24]; $t(35) = 3.60$, $p < .001$, see also Fig. 4b).

313



314

315 Fig. 4. Comparison of semi-partial correlations with smoothed human fixations for (a) MMs
316 and GBVS and for (b) MMs and DGII. The obtained coefficients were significantly higher when
317 assessing MMs while controlling for GBVS compared to when assessing GBVS when
318 controlling for MMs. The opposite was true for the analyses with DGII. All figure
319 characteristics are as in Fig. 3. except that medians instead of means are presented.

320

Pedziwiatr et al.

321 **Internal replication.** To demonstrate the generalizability of our conclusions beyond SCEGRAM
322 images, we replicated the main results with a different stimulus set (see the Supplement).

323

324 **Comparing meaning maps and saliency models – discussion**

325 If human gaze is guided by meaning, and if MMs index the distribution of meaning across an
326 image, MMs should outperform saliency models that are exclusively based on image features.
327 Our first analysis showed that this prediction does not hold. In fact, DGII generated better
328 predictions and explained more unique variance than MMs. Therefore, at least one of the two
329 premises of our prediction is wrong: either human eye-movements are not sensitive to
330 meaning or MM do not index meaning. The second analysis allowed us to distinguish between
331 these alternatives.

332

333 **Analyzing the effects of semantic inconsistencies within scenes – method**

334 In the second analysis, we assessed how human observers, DGII, and MMs respond to
335 experimental changes in meaning induced by altered object-context relationships. We used
336 eye-movement data from both the Consistent and the Inconsistent condition. These
337 conditions differed solely in the Critical Region, an area that either contained an object that
338 was either consistent with the scene context or induce semantic conflict. For each scene, we
339 calculated the mass of the distributions of human gaze, DGII, and MMs falling into the Critical
340 Region, respectively, and divided it by the Region's area for normalization. Our primary
341 interest was the comparison between conditions: to the extent to which humans, DGII, and
342 MMs are sensitive to meaning, they should fixate more (humans) or predict more fixations
343 (DGII and MMs) on the Critical Region in the Inconsistent than the Consistent condition.

344

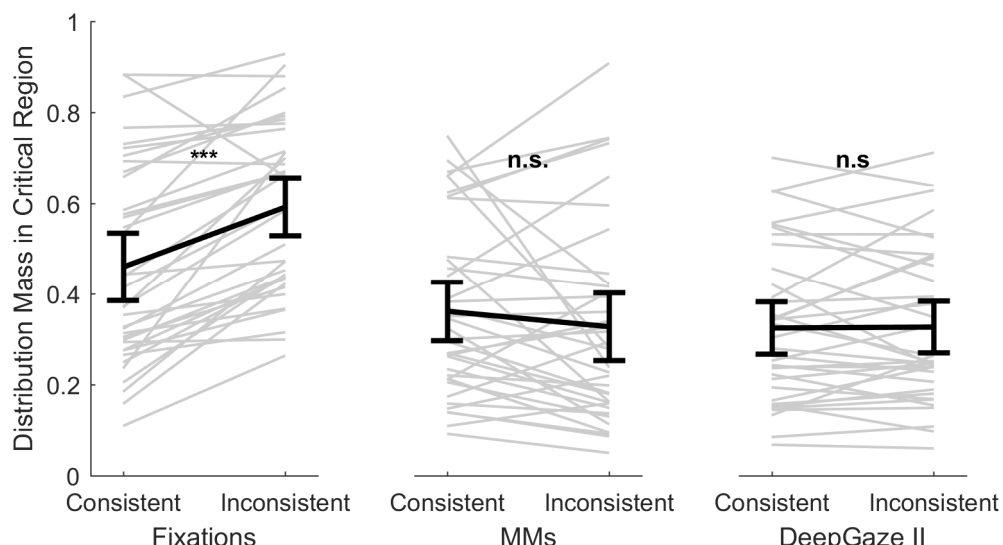
345 **Analyzing the effects of semantic inconsistencies within scenes – results**

346 Our comparison indicated that, as predicted, observers fixated more on inconsistent than
347 consistent objects (Fig. 5a). By contrast, behavior of both MMs and DGII did not change across
348 conditions (Fig. 5b and c). These impressions were confirmed by a 2x3 ANOVA, with condition

Pedziwiatr et al.

349 (Consistent vs. Inconsistent) as a within-subjects factor and the distribution source (human
350 fixations vs. MMs vs. DGII) as a between-subjects factor. We found a statistically significant
351 main effect of distribution source, $F(2, 105) = 13.09$, $p < .001$, $\omega^2 = 0.16$ and condition, $F(1,$
352 $105) = 7.41$ $p = 0.0076$ \times , $\omega^2 = 0.005$. These main effects were qualified by a significant
353 interaction, $F(2, 105) = 16.90$, $p < .001$ \times , $\omega^2 = 0.026$. Tukey post-hoc tests showed that human
354 observers looked more at the Critical Regions in the Inconsistent, than the Consistent
355 condition, $t(105) = -6.22$, $p < .001$. In contrast, no significant differences between conditions
356 were found for DGII, $t(105) = -0.09$ $p = 1.0$, and MMs, $t(105) = 1.60$ $p = 0.6028$. Comparisons
357 within conditions indicated that human fixations differed from MMs in the Inconsistent
358 condition, $t(129.91) = 5.78$ $p < .001$, but not the Consistent condition, $t(129.91) = 2.16$ $p =$
359 0.2662. A significant difference between DGII and human fixations was detected in both
360 Consistent, $t(129.91) = -2.96$ $p = 0.0420$, and Inconsistent conditions, $t(129.91) = -5.79$ $p <$
361 $.001$.

362



364 Fig. 5. Normalized distribution mass falling within Critical Regions in both conditions for (a)
365 smoothed human fixations, (b) MMs, and (c) DGII. All figure characteristics are as in Fig. 3.

366

367 Additionally, conditions differed regarding the number of fixations per image, $t(35) = 5.67$ p
368 $< .001$. On average, there were 6% fewer fixations in the Inconsistent condition. This excludes

Pedziwiatr et al.

369 the possibility that higher number of fixations in this condition might drive the observed
370 increase in the distribution mass falling within the Critical Regions.

371 Finally, systematic differences in object size between Consistent and Inconsistent conditions
372 could affect our results because larger objects may attract more fixations solely because they
373 occupy a larger image area. However, this factor was minimized by showing each object in a
374 consistent and an inconsistent context. Yet, the same object might be shown in a slightly
375 different position in the two conditions and might therefore occupy slightly different amounts
376 of the image. This was, however, not the case: the JZS Bayes Factor of 4.26 indicated that the
377 two conditions did not differ in the size of the bounding boxes of each manipulated object
378 (objects in the Inconsistent condition were on average 1562.28 pixels larger; 95% confidence
379 interval: [-2582.74, 5707.29]).

380 To summarize, semantic changes induced by altering object-context relationships elicited
381 changes in distributions of human fixations, but neither MMs nor DGII could predict them.
382 These results suggest that both models might be sensitive to image features, which are
383 frequently correlated with image meaning, rather than to meaning itself.

384

385 Discussion

386 A long-standing debate in visual perception concerns the extent to which visual features vs.
387 semantic content guide human eye-movements in free viewing of natural scenes. To
388 distinguish these hypotheses, indexing the distributions both of features and meaning across
389 an image is critical. While image-based saliency models have been used to index features for
390 two decades, measuring semantic importance has been difficult until meaning maps (MMs)
391 have recently been proposed. Here, we assessed the extent to which MMs indeed capture
392 the distribution of meaning across an image. First, we demonstrate that despite the
393 purported importance of meaning as measured by MMs for gaze control, MMs are not better
394 predictors of locations of human fixations than at least some saliency models, which are based
395 solely on image features. In fact, DeepGaze II (DGII), a model using deep neural network
396 features, outperformed MMs. Second, we assessed the sensitivity of human eye-movements,
397 MMs, and DGII to changes in image meaning induced by violations of typical object-context

Pedziwiatr et al.

398 relationships. Observers fixated more often on regions containing objects inconsistent with
399 scene context (thus replicating previous findings) but these regions were not indexed as more
400 meaningful by MMs, or as more salient by DGII. Together, these findings challenge central
401 assumptions of MMs, suggesting that they are insensitive to the semantic information
402 contained in the stimulus.

403 The good performance of DGII in predicting human gaze might be attributable to the high-
404 level features it extracts from images. Three other models, which use low-level features,
405 failed to decisively outperform MMs. However, unlike two of them (GBVS and AWS), DGII is
406 trained with data on human fixations to optimize performance (Kümmerer et al., 2016, 2017).
407 Yet, training alone cannot explain the difference in performance. The third low-level feature
408 model (ICF) is trained in the same way (Kümmerer et al., 2017) but still achieves a lower
409 performance than DGII. These findings suggest that feature type is indeed critical for a
410 model's performance. Importantly, however, while DGII uses high-level features transferred
411 from a deep neural network trained on object recognition (Simonyan & Zisserman, 2014), this
412 is not equivalent to indexing meaning. Rather, the good performance of DGII is likely due to
413 meaning supervening on, or correlating with, some of the features indexed by this model.

414 Correlation between visual features and meaning as the source of good performance in
415 saliency models has already been considered by the authors of MMs (Henderson & Hayes,
416 2017). Our findings suggest that MMs might share this characteristic with saliency models.
417 Specifically, the ratings used to construct MMs might be based on visual properties in such a
418 way that highly structured patches that contain high-level features receive high ratings. These
419 features often correlate with meaning, but in and of themselves do not amount to meaning.
420 According to this interpretation, both DGII and MMs index high-level features. Their success
421 in predicting human behavior derives from the typically strong correlation between high-level
422 features and meaning, with a higher correlation for the features extracted by DGII than MMs.

423 An alternative interpretation of the finding that DGII outperforms MMs is that image features
424 rather than meaning guide human fixations. However, this interpretation is inconsistent with
425 our second analysis. Here, observers clearly exhibited sensitivity to meaning, as indicated by
426 changed gaze patterns after introducing semantic inconsistencies into the scenes. This
427 experimental manipulation targets a type of meaning that is based on how objects relate to
428 the broader context in which they occur. While specific, it is precisely this kind of meaning

Pedziwiatr et al.

429 that is of high theoretical importance in eye-movement research (Henderson, 2017;
430 Henderson et al., 2009). Thus, even if MMs were to measure other types of meaning, as has
431 been suggested (Henderson et al., 2018), the fact that they are not sensitive to meaning
432 derived from object-context relationships seriously limits their usefulness. Moreover, the idea
433 that MMs indeed index other kinds of meaning that are important for guidance of fixations is
434 not consistent with our findings. If this were the case, then we would expect MMs to predict
435 human fixations better than saliency models that solely rely on image features, which is not
436 the case.

437 The insensitivity to semantic inconsistencies reveals inherent limitations of both MMs and
438 DGII. The way in which MMs are constructed implicitly assumes that meaning is a local image-
439 property, which is not true for object-context (in)consistency. This limitation may potentially
440 be alleviated by 'contextualized MMs' (Peacock, Hayes, & Henderson, 2019), a recently
441 suggested modification of the 'standard' MMs. These novel maps are created from
442 meaningfulness ratings by observers who see the whole scenes from which the to-be-rated
443 patches were derived. It is yet to be seen what this approach can reveal about fixation
444 selection beyond the fact that humans asked to indicate meaningful or interesting regions
445 within scenes highlight areas, which tend to be frequently fixated by other observers
446 (Nyström & Holmqvist, 2008; Onat et al., 2014). DGII, in turn, does not explicitly encode
447 semantic information, and was not trained on the relationship between eye movements and
448 semantic (in)consistency. But its failure highlights an opportunity to improve saliency models
449 by incorporating semantic relationships (Bayat, Koh, Nand, Pereira, & Pomplun, 2018).

450 Taken together, our results suggest that, contrary to their core promise as a methodology,
451 meaning maps (MMs) do not offer a way to measure the spatial distribution of meaning across
452 an image. Instead of meaning per-se, they seem to index high-level features that have the
453 potential to carry meaning in typical natural scenes. They share this characteristic with state-
454 of-the-art saliency models, which are easier to use, do not require human annotation, and yet
455 predict locations of human fixations better than MMs.

456

457

458

Pedziwiatr et al.

459

Author contributions

460 C.T. and M.P. conceived of the study. M.P., T.W., and C.T. designed the experiment. M.P.
461 collected and analyzed the data under the supervision of C.T. with support from M.K., T.W.,
462 and M.B. The paper was drafted by M.P. and C.T.; T.W., M.K., and M.B. provided detailed
463 comments.

464

465

References

466 Bayat, A., Koh, D. H., Nand, A. K., Pereira, M., & Pomplun, M. (2018). Scene Grammar in
467 Human and Machine Recognition of Objects and Scenes. In *Proceedings of the IEEE*
468 *Conference on Computer Vision and Pattern Recognition Workshops*.
469 <https://doi.org/10.1109/CVPRW.2018.00268>

470 Borji, A., Sihite, D. N., & Itti, L. (2013). Objects do not predict fixations better than early
471 saliency : A re-analysis of Einhäuser et al.'s data. *Journal of Vision*, 13(2013), 1–4.
472 <https://doi.org/10.1167/13.10.18>

473 Bylinskii, Z., Judd, T., Borji, A., Itti, L., Durand, F., Oliva, A., & Torralba, A. (2014). MIT Saliency
474 Benchmark Results. Retrieved from <http://saliency.mit.edu/>

475 Bylinskii, Z., Judd, T., Oliva, A., Torralba, A., & Durand, F. (2016). What do different
476 evaluation metrics tell us about saliency models? *ArXiv*. Retrieved from
477 <http://arxiv.org/abs/1604.03605>

478 Garcia-Díaz, A., Fdez-Vidal, X. R., Pardo, X. M., & Dosil, R. (2012). Saliency from hierarchical
479 adaptation through decorrelation and variance normalization. *Image and Vision
480 Computing*, 30(1), 51–64. <https://doi.org/10.1016/j.imavis.2011.11.007>

481 Harel, J., Koch, C., & Perona, P. (2006). Graph-Based Visual Saliency. *Advances in Neural
482 Information Processing Systems* 19, 19, 545–552. <https://doi.org/10.1.1.70.2254>

483 Hayes, T. R., & Henderson, J. M. (2019). Center bias outperforms image salience but not
484 semantics in accounting for attention during scene viewing. *Attention, Perception, &
485 Psychophysics*. <https://doi.org/https://doi.org/10.3758/s13414-019-01849-7>

Pedziwiatr et al.

486 Hayhoe, M., & Ballard, D. (2005). Eye movements in natural behavior. *Trends in Cognitive
487 Sciences*, 9(4). <https://doi.org/10.1016/j.tics.2005.02.009>

488 Hegde, J., & Kersten, D. (2010). A Link between Visual Disambiguation and Visual Memory.
489 *Journal of Neuroscience*, 30(45), 15124–15133.
490 <https://doi.org/10.1523/JNEUROSCI.4415-09.2010>

491 Henderson, J. M. (2017). Gaze Control as Prediction. *Trends in Cognitive Sciences*, 21(1), 15–
492 23. <https://doi.org/10.1016/j.tics.2016.11.003>

493 Henderson, J. M., & Hayes, T. R. (2017). Meaning-based guidance of attention in scenes as
494 revealed by meaning maps. *Nature Human Behaviour*, 1(October).
495 <https://doi.org/10.1038/s41562-017-0208-0>

496 Henderson, J. M., & Hayes, T. R. (2018). Meaning guides attention in real-world scene
497 images: Evidence from eye movements and meaning maps. *Journal of Vision*, 18(6), 10.
498 <https://doi.org/10.1167/18.6.10>

499 Henderson, J. M., Hayes, T. R., Peacock, C. E., & Rehrig, G. (2019). Meaning and Attentional
500 Guidance in Scenes : A Review of the Meaning Map Approach. *Vision*, 3(2).

501 Henderson, J. M., Hayes, T. R., Rehrig, G., & Ferreira, F. (2018). Meaning Guides Attention
502 during Real-World Scene Description. *Scientific Reports*, 8(1), 13504.
503 <https://doi.org/10.1038/s41598-018-31894-5>

504 Henderson, J. M., Malcolm, G. L., & Schandl, C. (2009). Searching in the dark: Cognitive
505 relevance drives attention in real-world scenes. *Psychonomic Bulletin & Review*, 16(5),
506 850–856. <https://doi.org/10.3758/PBR.16.5.850>

507 Henderson, J. M., Weeks, P. A., & Hollingworth, A. (1999). The effects of semantic
508 consistency on eye movements during complex scene viewing. *Journal of Experimental
509 Psychology: Human Perception and Performance*, 25(1), 210–228.
510 <https://doi.org/10.1037/0096-1523.25.1.210>

511 Itti, L., & Koch, C. (2000). A saliency-based search mechanism for overt and covert shifts of
512 visual attention. *Vision Research*, 40(10–12), 1489–1506.
513 [https://doi.org/10.1016/S0042-6989\(99\)00163-7](https://doi.org/10.1016/S0042-6989(99)00163-7)

Pedziwiatr et al.

514 Itti, L., & Koch, C. (2001). Computational modelling of visual attention. *Nature Reviews Neuroscience*, 2(3), 194–203. <https://doi.org/10.1038/35058500>

515

516 Kietzmann, T. C., McClure, P., & Kriegeskorte, N. (2019). Deep Neural Networks in
517 Computational Neuroscience. In *Oxford Research Encyclopedia of Neuroscience*.

518 Kleiner, M., Brainard, D., & Pelli, D. G. (2007). What's new in psychtoolbox-3? *Perception*,
519 36(1).

520 Koehler, K., Guo, F., Zhang, S., & Eckstein, M. P. (2014). What do saliency models predict?
521 *Journal of Vision*, 14(3). <https://doi.org/10.1167/14.3.14>

522 Kümmerer, M., Wallis, T. S. A., & Bethge, M. (2015). Information-theoretic model
523 comparison unifies saliency metrics. *Proceedings of the National Academy of Sciences*,
524 112(52), 16054–16059. <https://doi.org/10.1073/pnas.1510393112>

525 Kümmerer, M., Wallis, T. S. A., & Bethge, M. (2016). DeepGaze II: Reading fixations from
526 deep features trained on object recognition, 1–16. Retrieved from
527 <http://arxiv.org/abs/1610.01563>

528 Kümmerer, M., Wallis, T. S. A., & Bethge, M. (2018). Saliency Benchmarking Made Easy:
529 Separating Models, Maps and Metrics. In V. Ferrari, M. Hebert, C. Sminchisescu, & Y.
530 Weiss (Eds.), *Computer Vision – ECCV 2018. ECCV 2018. Lecture Notes in Computer
531 Science* (Vol. 11220, pp. 798–814). Springer. https://doi.org/10.1007/978-3-030-01270-0_47

533 Kümmerer, M., Wallis, T. S. A., Gatys, L. A., & Bethge, M. (2017). Understanding Low- and
534 High-Level Contributions to Fixation Prediction. In *The IEEE International Conference on
535 Computer Vision (ICCV)*. <https://doi.org/10.1109/ICCV.2017.513>

536 Nyström, M., & Holmqvist, K. (2008). Semantic override of low-level features in image
537 viewing—both initially and overall. *Journal of Eye Movement Research*, 2(2), 1–11.
538 <https://doi.org/10.16910/jemr.2.2.2>

539 Öhlschläger, S., & Võ, M. L. H. (2017). SCEGRAM: An image database for semantic and
540 syntactic inconsistencies in scenes. *Behavior Research Methods*, 49(5).
541 <https://doi.org/10.3758/s13428-016-0820-3>

Pedziwiatr et al.

542 Onat, S., Açık, A., Schumann, F., & König, P. (2014). The contributions of image content and
543 behavioral relevancy to overt attention. *PLoS ONE*, 9(4).
544 <https://doi.org/10.1371/journal.pone.0093254>

545 Parkhurst, D., Law, K., & Niebur, E. (2002). Modeling the role of salience in the allocation of
546 overt visual attention. *Vision Research*, 42(1), 107–123. [https://doi.org/10.1016/S0042-6989\(01\)00250-4](https://doi.org/10.1016/S0042-6989(01)00250-4)

548 Peacock, C. E., Hayes, T. R., & Henderson, J. M. (2018). Meaning guides attention during
549 scene viewing, even when it is irrelevant. *Attention, Perception, and Psychophysics*, 20–
550 34. <https://doi.org/10.3758/s13414-018-1607-7>

551 Peacock, C. E., Hayes, T. R., & Henderson, J. M. (2019). The role of meaning in attentional
552 guidance during free viewing of real-world scenes. *Acta Psychologica*, 198(June).
553 <https://doi.org/10.1016/j.actpsy.2019.102889>

554 Rider, A. T., Coutrot, A., Pellicano, E., Dakin, S. C., & Mareschal, I. (2018). Semantic content
555 outweighs low-level saliency in determining children's and adults' fixation of movies.
556 *Journal of Experimental Child Psychology*, 166, 293–309.
557 <https://doi.org/10.1016/j.jecp.2017.09.002>

558 Rouder, J. N., Speckman, P. L., Sun, D., Morey, R. D., & Iverson, G. (2009). Bayesian t tests for
559 accepting and rejecting the null hypothesis. *Psychonomic Bulletin and Review*, 16(2),
560 225–237. <https://doi.org/10.3758/PBR.16.2.225>

561 Simonyan, K., & Zisserman, A. (2014). Very Deep Convolutional Networks for Large-Scale
562 Image Recognition. *CoRR, Abs/1409.1556*. Retrieved from
563 <http://arxiv.org/abs/1409.1556>

564 Stoll, J., Thrun, M., Nuthmann, A., & Einhäuser, W. (2015). Overt attention in natural scenes:
565 Objects dominate features. *Vision Research*, 107, 36–48.
566 <https://doi.org/10.1016/j.visres.2014.11.006>

567 Tatler, B. (2007). The central fixation bias in scene viewing: Selecting an optimal viewing
568 position independently of motor biases and image feature distributions. *Journal of*
569 *Vision*, 7(4), 1–17. <https://doi.org/10.1167/7.14.4>

Pedziwiatr et al.

570 Tatler, B. W., Hayhoe, M. M., Land, M. F., & Ballard, D. H. (2011). Eye guidance in natural
571 vision: Reinterpreting salience. *Journal of Vision*, 11(5), 5–5.
572 <https://doi.org/10.1167/11.5.5>

573 Teufel, C., Dakin, S. C., & Fletcher, P. C. (2018). Prior object-knowledge sharpens properties
574 of early visual feature- detectors. *Scientific Reports*, (June), 1–12.
575 <https://doi.org/10.1038/s41598-018-28845-5>

576 Zhang, L., Tong, M. H., Marks, T. K., & Cottrell, G. W. (2008). SUN: A Bayesian framework for
577 saliency using natural statistics. *Journal of Vision*, 8(32). <https://doi.org/10.1167/8.7.32>

578